
Auto-Spikformer: Spikformer Architecture Search

Kaiwei Che^{1,2}, Zhaokun Zhou^{1,2}, Zhengyu Ma², Wei Fang^{1,2},
Yanqi Chen^{1,2}, Shuaijie Shen³, Li Yuan^{1,2*}, Yonghong Tian^{1,2*}

¹ Peking University, China

² Peng Cheng Laboratory, China

³ Southern University of Science and Technology, China

Abstract

The integration of self-attention mechanisms into Spiking Neural Networks (SNNs) has garnered considerable interest in the realm of advanced deep learning, primarily due to their biological properties. Recent advancements in SNN architecture, such as Spikformer, have demonstrated promising outcomes by leveraging Spiking Self-Attention (SSA) and Spiking Patch Splitting (SPS) modules. However, we observe that Spikformer may exhibit excessive energy consumption, potentially attributable to redundant channels and blocks. To mitigate this issue, we propose Auto-Spikformer, a one-shot Transformer Architecture Search (TAS) method, which automates the quest for an optimized Spikformer architecture. To facilitate the search process, we propose methods Evolutionary SNN neurons (ESNN), which optimizes the SNN parameters, and apply the previous method of weight entanglement supernet training, which optimizes the Vision Transformer (ViT) parameters. Moreover, we propose an accuracy and energy balanced fitness function \mathcal{F}_{AEB} that jointly considers both energy consumption and accuracy, and aims to find a Pareto optimal combination that balances these two objectives. Our experimental results demonstrate the effectiveness of Auto-Spikformer, which outperforms the state-of-the-art method including CNN or ViT models that are manually or automatically designed while significantly reducing energy consumption.

1 Introduction

Spiking neural networks (SNNs) are promising for the next generation of artificial intelligence due to their biological inspiration and appealing features such as sparse activation and temporal dynamics. The performance of SNNs has improved by utilizing advanced architectures from ANNs such as ResNet-like SNNs [25, 17, 75, 26] or Spiking Recurrent Neural Networks [39]. Transformer, originally developed for natural language processing[57], has been successful in a variety of computer vision applications, including image classification[15, 71], object detection [3, 77, 38], semantic segmentation [59, 72]. The self-attention mechanism, a crucial component of the Transformer model, selectively attends to relevant information and is analogous to an important feature of the human biological system [62, 4]. The integration of self-attention into SNN for advanced deep learning has gained attention due to the biological properties of both mechanisms. Spikformer [76], a recent SNN architecture, has demonstrated promising results on both static and neuromorphic datasets using its Spiking Self-Attention (SSA) and Spiking Patch Splitting (SPS) modules.

Although SNNs are known for their low energy consumption compared to ANN, our observations revealed that the energy consumption of Spikformer can be significantly reduced as it contains potentially redundant channels and blocks. Through experimentation, with only fewer blocks and channels, we obtain even better accuracy. It motivates us to search for improved Spikformer architectures that balance energy consumption and accuracy. Nevertheless, designing and training

*Corresponding authors.

such hybrid models remains a challenging task [15, 56]. Transformer Architecture Search (TAS) [6, 7, 55] gains attention as an automated way to search for multiple configurations of Vision Transformer (ViT) architectures. The one-shot NAS scheme [7, 14] is leveraged in TAS and obtains reliable performance estimations on various ViT architectures. The utilization of the one-shot NAS scheme, as proposed by [7, 14], is employed in the TAS and has proven to yield dependable performance estimations for diverse ViT architectures. Nevertheless, our experimental findings suggest that directly applying TAS may not be the most optimal solution for SNN. The original TAS method do not care about the SNN search space and the energy consumption, which is vital in the field of SNN.

To address this gap, we further analyze the two components of Spikformer: the Transformer architecture and SNN neurons. There are numerous prior methodologies proposed to optimize the Transformer architecture search, presenting various approaches that can be leveraged to achieve optimization. As to SNN neurons, the performance of an SNN neuron is determined by its internal parameters and interconnections. The Transformer component can also be regarded as the interconnections of SNN neurons in Spikformer. Several studies have focused on improving SNN performance by exploring the network’s structure [30, 5, 41]. However, the internal parameters of individual neurons have also been identified as important. In this study, we propose a method to investigate the optimization of both the internal parameters of individual neurons and the interconnections between neurons. SNN neurons are mathematical models that approximate the behavior of biological neurons. Changes in the internal structure of biological neurons are derived from their adaptation to the environment, which is very similar to Darwin’s theory of evolution [28, 53], which suggests that living organisms adapt to their environment over time through natural selection. According to this theory, individuals with traits that are advantageous for survival in a particular environment are more likely to survive and reproduce, passing on their advantageous traits to their offspring. In the context of SNN neurons, this concept of natural selection can be applied to the evolution of individual neurons. Specifically, the threshold u_{th} , decay τ , and time-step t parameters of a neuron can be regarded as its traits, while the input stimuli it receives can be considered as the environment in which it operates. Applying the concept of natural selection, the optimization of these parameter sets through simulated evolution may lead to improved network performance, resulting in increased accuracy and efficiency. Our study is the first to apply the evolutionary algorithm to search for the internal parameters of SNN neurons.

The energy consumption of Spikformer is influenced by several factors, such as the input image size, embedding dimension, number of blocks, firing rate, and time-step. Modifying the transformer architecture and selecting appropriate SNN parameters can adjust these factors. In evolutionary search, the fitness function is employed to evaluate candidate architectures. In order to achieve a balanced trade-off between energy consumption and accuracy, we incorporate energy as part of the fitness function. To the end, we propose a search space that considers both the original factors from the ViT and the additional factors from the SNN. Subsequently, we introduce a joint fitness function \mathcal{F}_{AEB} that takes into account both energy consumption and accuracy in order to optimize this extended search space. This approach allows us to obtain a Pareto optimal combination of energy consumption and accuracy, striking an optimal balance between the two objectives.

In summary, our contributions are following:

- To the best of our knowledge, this study is the first to use NAS for spiking-based ViT namely Auto-Spikformer. By using Evolutionary SNN neurons (ESNN) and weight entanglement [7] supernet training method, Auto-Spikformer enhances the efficiency and accuracy of spiking-based ViT architectures.
- Auto-Spikformer integrates an accuracy and energy balanced fitness function \mathcal{F}_{AEB} , to optimize the Spikformer search space by considering both energy consumption and accuracy simultaneously.
- Auto-Spikformer has been successfully searched and evaluated on the CIFAR dataset, achieving state-of-the-art results when compared to other SNN models in both accuracy and energy consumption.

2 Related work

2.1 Vision Transformer

The Vision Transformer (ViT) facilitates the transformation from the NLP to the CV by partitioning visual information into patches and processing it accordingly. Regarding the task of image classification, a Transformer encoder is comprised of a patch splitting module, multiple Transformer encoder blocks, and a linear prediction head. In each Transformer encoder block, there exists a self-attention layer along with a multi perception layer. Self-attention serves as the fundamental component contributing to the success of ViT. It enables the capture of global dependence and interest representation by weighing the feature values of image patches via the dot product of the query and key, followed by the application of the softmax function[29, 46]. Researchers have made several improvements to the visual transformer, including the Transformer architecture[66, 22], more advanced self-attention mechanisms[54, 68, 47, 11], and pre-training techniques[23], among others.

2.2 One Shot NAS

Designing high performance network architectures for specific tasks often requires expert experience and trial-and-error experiments. Neural architecture search (NAS) [16] aims to automate this manual process and has recently achieved highly competitive performance in tasks such as image classification [78, 79, 35, 51, 45], object detection [79, 9, 58, 20] and semantic segmentation [36, 74, 43, 34], etc. However, searching over a discrete set of candidate architectures often results in a massive number of potential combinations, leading to explosive computation cost. The recently proposed differentiable architecture search (DARTS) method [37] and its variations [67, 8, 12] address this problem using a continuous relaxation of the search space which enables learning a set of architecture coefficients by gradient descent, and has achieved competitive performances with the state-of-the-art using orders of magnitude fewer computation resources [37, 36, 10]. Recently, [41] studied pooling operations for downsampling in SNNs and applied NAS to reduce the the overall number of spikes. [30] applied NAS to improve SNN initialization and explore backward connections. However, both works only searched for different SNN cells or combinations of them under fixed network backbone and their application is limited to image classification.

2.3 Spiking Neural Networks

Unlike traditional deep learning models that perform computations using floating-point values, SNNs leverage discrete spike sequences for information processing and transmission. Spiking neurons endow SNNs with temporal dynamics and biological properties, with common types including including the leaky integrate-and-fire (LIF) neuron [63], PLIF [18], etc. There are two main approaches for obtaining deep SNNs: ANN-to-SNN conversion and direct training. In ANN-to-SNN conversion, a pre-trained ANN with high performance is transformed into an SNN by substituting the ReLU activation layers with spiking neurons[2, 27, 52, 1, 40, 60]. However, this method requires large time-steps to approximate ReLU activation accurately, which leads to high latency [21]. In direct training, SNNs are trained by backpropagation through time (BPTT)[61]. A challenge for direct training is the non-differentiability of the event-triggered mechanism in spiking neurons. To address this challenge, surrogate gradients are employed for backpropagation [33, 42, 65] adopts implicit differentiation on the equilibrium state to train SNNs.

3 Auto-Spikformer

3.1 LIF

We adopt the iterative LIF neuron model [64] described by

$$u^{t,n} = \left(1 - \frac{1}{\tau}\right)u^{t-1,n}(1 - y^{t-1,n}) + I^{t,n} \quad (1)$$

where superscripts n and t denote layer index and time-step, respectively. decay τ is the membrane time constant, u is the membrane potential, y denotes the spike output and I denotes the synaptic input with $I^{t,n} = \sum_j w_j y_j^{t,n-1}$ where w is the weight. The neuron will fire a spike $y^{t,n} = 1$ when $u^{t,n}$ exceeds a threshold V_{th} , otherwise $y^{t,n} = 0$. In this work, we set $\tau = 2$ and $u_{th} = 0.5$.

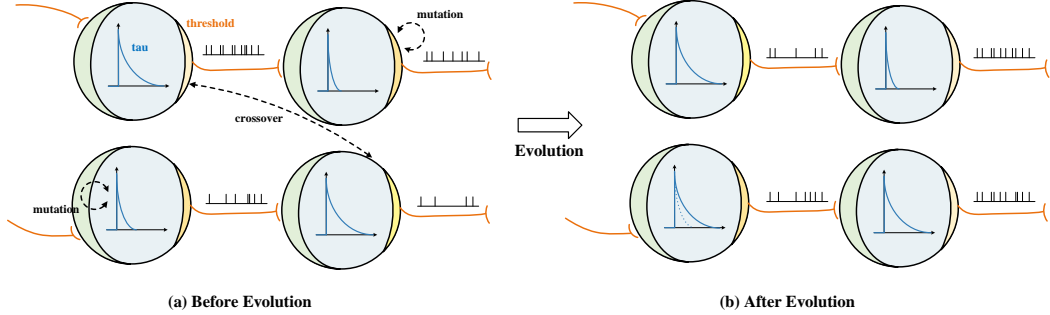


Figure 1: ESNN process. (a), (b) shows two candidate parameter sets before and after applying the mutation and crossover operators. The spike from the previous neuron is transmitted to the current neuron as the charging process. If the membrane potential is above the threshold (yellow area, where the darker color indicates a higher value), a spike is delivered, and if the membrane potential is below the threshold, it decays exponentially with a time constant τ (blue curve).

Table 1: Auto-Spikformer search space. \mathcal{S}_{T_s} denotes transformer smaller search space, \mathcal{S}_{T_l} denotes transformer larger search space, and \mathcal{S}_S denotes SNN search space. Each element in the table represents the lower limit, upper limit and step size, such as depth (2,4,1) represents the search space is [2,3,4]

	\mathcal{S}_{T_s}	\mathcal{S}_{T_l}	\mathcal{S}_S	
embed dim	(336,384,12)	(336,480,48)	threshold u_{th}	(0.6,2,0.2)
MLP ratio	(3,4,0.2)	(3,5,0.2)	decay τ	(1.25,10,0.25)
head num	(6,12,6)	(6,12,6)	time-step t	(2,4,1)
depth	(2,4,1)	(2,6,1)		

(a) CIFAR search space

(b) SNN search space

3.2 Evolutionary SNN Neurons (ESNN)

The performance of SNN neurons is influenced by both their interconnections and internal parameters. While previous research has primarily focused on enhancing SNN performance through modifications to the network’s structure, the importance of optimizing the internal parameters within individual neurons cannot be overlooked. Darwin’s theory of evolution posits that organisms adapt to their surroundings through natural selection, favoring traits that enhance survival and reproduction. This concept can be applied to the context of SNN, where individual neurons can undergo an evolutionary process. In this context, the internal parameters of a neuron, such as the threshold (u_{th}), decay (τ), and time-step (t), can be seen as analogous to traits, while the input stimuli received by the neuron can be likened to the environment in which it operates.

Previous work [19] suggests that the threshold can be viewed as an adaptation to membrane potentials at short timescales, influencing how signals received by a neuron are encoded into a spike. Decay τ has a similar effect to the threshold, but it only affects the decay of unfired neurons, influencing the firing of the next timestep. In contrast, the threshold affects the firing of all neurons at the current moment.

As shown in Figure 1, the spike from the previous neuron is transmitted to the current neuron as the charging process. If the membrane potential is above the threshold, a spike is delivered, and if the membrane potential is below the threshold, it decays at the rate of τ . The ESNN begins with a population of randomly generated parameter sets (candidates) like [$u_{th} = 1.2, \tau = 1.25, t = 4$]. In each generation, the algorithm evaluates the fitness of candidates and selects the best ones as the parents for the next generation. The parents produce offspring by applying mutation and crossover operators with some probabilities. The mutation operator randomly modifies one parameter of a parameter set, while the crossover operator combines two parameters from different parents. As illustrated in Figure 2, for example, the decay τ of a candidate changes from 1.25 to 2.5 after mutation. the thresholds u_{th} of two candidates are swapped after crossover, which affects the firing rate of each

candidate. The algorithm repeats this process for a fixed number of generations and returns the best architecture found. Through a process of simulated evolution, the threshold, decay, and time-step parameters of individual neurons can be adjusted to improve the performance of the network as a whole. According to our experiments, this approach can lead to the network becoming better adapted to the input stimuli it receives, resulting in increased accuracy and efficiency.

Specifically, we design a SNN search space denoted \mathcal{S}_S that includes three variable factors: the threshold u_{th} , decay τ , and time-step t . The structured definition of this search space is outlined in Table 1 (b), and its visual interpretation is depicted in Figure 1. To conduct this exploration, we adopt a supernet-based approach inspired by one-shot NAS methods, where all subnets share the same weights as the supernet, and only the SNN variable factors differ. Our process begins with the generation of an initial set of candidate parameter sets using a random search. More details about the selection process are in the supplement.

3.3 Accuracy and Energy Balanced Fitness Function (\mathcal{F}_{AEB})

In this study, we apply a large transformer search space that includes four variable factors to increase model capacities, similarly to the Autoformer [7]. We encode the search space into a supernet. However, the original fitness function only takes accuracy into account. We propose a new fitness function \mathcal{F}_{AEB} that can balance the accuracy and the energy consumption. To estimate the energy use, we need to compute the synaptic operations (SOPs) first. For a specific layer l , its SOPs can be calculated as follows,

$$\text{SOPs}(l) = fr \times t \times \text{FLOPs}(l) \quad (2)$$

where fr denotes the firing rate of the input spike train, t represents time-step. Floating Point Operations (FLOPs) refer to the number of multiply-and-accumulate (MAC) operations. And SOPs contain spike-based accumulate (AC) operations only. We estimate the theoretical energy consumption of Auto-Spikformer according to [32, 26, 24, 31, 70, 44, 69]. We assume that the MAC and AC operations are implemented on the 45nm CMOS technology [49], where $E_{MAC} = 4.6pJ$ and $E_{AC} = 0.9pJ$. The theoretical energy consumption of Auto-Spikformer is calculated:

$$\begin{aligned} \mathcal{E} = & E_{MAC} \times \text{FL}_{\text{SNN Conv}}^1 \\ & + E_{AC} \times \left(\sum_{n=2}^N \text{SOP}_{\text{SNN Conv}}^n + \sum_{m=1}^M \text{SOP}_{\text{SNN FC}}^m + \sum_{l=1}^L \text{SOP}_{\text{SSA}}^l \right) \end{aligned} \quad (3)$$

where \mathcal{E} denotes the model energy, $\text{FL}_{\text{SNN Conv}}^1$ is the first layer to encode static RGB images into spike-form. Then the SOPs of m SNN Conv layers, n SNN Fully Connected Layer (FC) and l SSA are added together and multiplied by E_{AC} . For ANNs, the theoretical energy consumption of block b is calculated:

$$\text{Power}(b) = 4.6pJ \times \text{FLOPs}(b) \quad (4)$$

For SNNs, $\text{Power}(b)$ is:

$$\text{Power}(b) = 0.9pJ \times \text{SOPs}(b) \quad (5)$$

The energy consumption of Spikformer is determined by multiple factors, including input image size, embedding dimension, number of blocks, firing rate fr , and time-step t . Most of these factors can be adjusted by changing the transformer architecture and selecting suitable spike neuron parameters. To facilitate comparison, we normalized these factors using a minmax scaler and assigned different weights to both metrics, the accuracy and energy balanced fitness function \mathcal{F}_{AEB} is described as follows.

$$\mathcal{F}_{AEB} = \alpha \times \mathcal{E} + (1 - \alpha) \times \mathcal{A} \quad (6)$$

where \mathcal{A} denotes the top-1 accuracy. Both of them are scaled by a minmax scaler and the range is (0,1). α denotes the weight. In our case, we set α to 0.5.

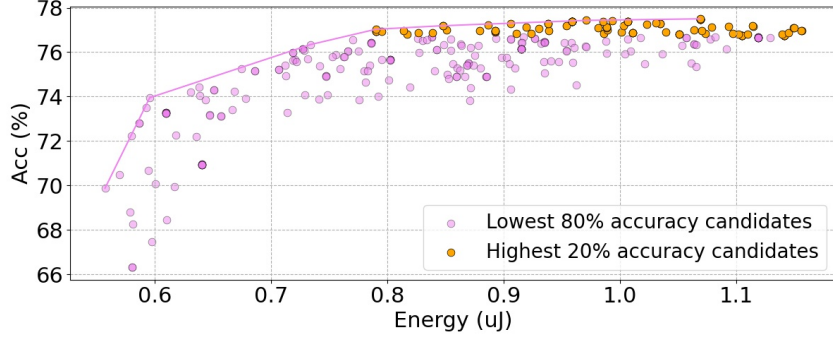


Figure 2: The energy and accuracy of all candidates in \mathcal{S}_S in CIFAR100. We use \mathcal{F}_{AEB} as the fitness function to select the top 300 candidates. The purple points represent the candidates with the lowest 80% accuracy, while the orange points represent the candidates with the highest 20% accuracy. The purple line represents the Pareto frontier, indicating the optimal trade-off between accuracy and energy consumption.

Table 2: Subsets of the candidates in \mathcal{S}_S . It should be noted that the last row corresponds to Spikformer 4-384, which was obtained by running the open-source code of Spikformer in Auto-Spikformer mode. Therefore, its weight differs from the other models in the table. The bold font represents that the energy consumption and accuracy are superior to Spikformer 4-384.

Candidates (threshold $\times 4, \tau \times 4$, time-step)	Fr	Energy (μJ)	Acc (%)	Candidates (threshold $\times 4, \tau \times 4$, time-step)	Fr	Energy (μJ)	Acc (%)
(1.6, 0.6, 0.8, 2.0, 10, 10, 10, 2, 2)	0.20	0.52	72.12	(1.0, 2.0, 1.6, 2.0, 5, 2, 2, 3, 4)	0.30	0.79	77.87
(1.8, 0.8, 1.4, 1.2, 10, 10, 10, 2, 2)	0.20	0.52	72.18	(1.2, 1.8, 1.8, 1.6, 2, 10, 1.5, 5, 4)	0.33	0.87	77.90
(1.6, 0.6, 2.0, 1.8, 5, 10, 10, 1.5, 4)	0.24	0.63	75.58	(1.6, 1.2, 1.8, 2.0, 1.5, 5, 10, 2, 4)	0.33	0.88	77.86
(1.0, 1.0, 1.4, 1.0, 10, 10, 2, 3, 4)	0.25	0.66	76.44	(1.6, 0.8, 1.2, 1.8, 2, 10, 1.25, 3, 4)	0.34	0.91	77.74
(1.8, 1.6, 0.6, 0.8, 5, 10, 2, 3, 4)	0.26	0.68	76.77	(0.6, 1.4, 1.2, 0.6, 2, 3, 1.25, 5, 4)	0.35	0.94	77.78
(0.8, 1.2, 1.6, 2.0, 5, 10, 2, 1.5, 4)	0.27	0.72	77.20	(0.8, 0.8, 1.8, 1.8, 2, 2, 1.5, 2, 3)	0.36	0.95	77.92
(1.0, 2.0, 1.6, 2.0, 5, 2, 2, 3, 4)	0.30	0.79	77.87	(1.0, 1.4, 1.8, 0.6, 2, 2, 1.5, 3, 4)	0.36	0.96	77.77
(1.0, 2.0, 1.4, 1.6, 2, 2, 1.25, 5, 4)	0.37	0.99	77.95	(1.0, 2.0, 1.4, 1.6, 2, 2, 1.25, 5, 4)	0.37	0.99	77.95
(1.0, 1.0, 1.0, 1.0, 2, 2, 2, 2, 4)	0.35	0.95	77.86	(1.0, 1.0, 1.0, 1.0, 2, 2, 2, 2, 4)	0.35	0.95	77.86

(a) Candidates on the Pareto frontier.

(b) Candidates with the top 20% accuracy.

4 Experiments

In this section, we provide a comprehensive overview of the implementation details and the settings used for the evolution search. Initially, we conduct an analysis to assess the effectiveness of the ESNN by focusing on modifications within the SNN search space. Subsequently, we evaluate the efficacy of the \mathcal{F}_{AEB} by comparing it with a random search approach and construct the Pareto frontier. Lastly, we present the performance evaluation of Auto-Spikformer on CIFAR dataset, providing comparisons with state-of-the-art models to highlight its effectiveness.

4.1 Implementation Details

Auto-Spikformer includes two stages: the supernet training stage and the evolutionary search stage. The implementation of all models utilized PyTorch 1.8 and the training process was performed on Nvidia Tesla V100 GPUs. Additional implementation details can be found in the supplementary materials. During the supernet training stage, we followed a similar training approach as Spikformer, but with an extended epoch duration of 1000 to ensure improved convergence of the supernet. Subsequently, in the evolutionary search stage, we adopted a similar protocol as SPOS and Autoformer for the implementation of the evolutionary search. Our approach involved employing ESNN to explore thousands of candidate architectures and SNN parameter sets. We conduct our experiments on CIFAR dataset. CIFAR provides 50,000 train and 10,000 test images with 32×32 resolution. The batch size is set to 128.

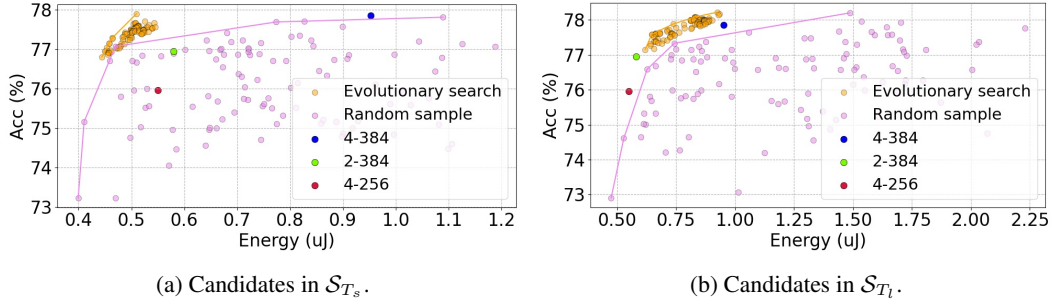


Figure 3: The energy and accuracy of all searched candidates in \mathcal{S}_{T_s} and \mathcal{S}_{T_l} in CIFAR100. We use \mathcal{F}_{AEB} as the fitness function (purple points) and randomly (orange points) select the 100 candidates, respectively. The other color points represent the different architectures of Spikformer, which are derived from the original paper [76].

Table 3: Subsets of the candidates in \mathcal{S}_S . The bold font represents that the energy consumption and accuracy are superior to Spikformer 4-384.

(a) Candidates in \mathcal{S}_{T_s} . We denotes ^{1,2} as Auto-Spikformer $\mathcal{S}_{T_s 1,2}$.

(b) Candidates in \mathcal{S}_{T_l} . We denotes ^{1,2,3} as Auto-Spikformer $\mathcal{S}_{T_l 1,2,3}$

	Candidates		Energy (μJ)	Acc (%)	Candidates		Energy (μJ)	Acc (%)
	(depth (d), MLP ratio \times d, head num \times d, threshold \times d, tau \times d, time-step, embed dim)				(depth (d), MLP ratio \times d, head num \times d, threshold \times d, tau \times d, time-step, embed dim)			
Pareto frontier	(2, 3.2, 3.0, 12, 6, 1.2, 1.0, 5, 5, 4, 348)	0.448	76.89	(2, 4.8, 3.2, 6, 6, 1.4, 1.6, 5, 5, 4, 384)	0.619	77.15		
	(2, 3.4, 3.2, 12, 6, 1.0, 1.0, 5, 5, 4, 348)	0.453	77.04	(2, 3.8, 3.2, 6, 12, 0.8, 1.2, 5, 5, 4, 432)	0.647	77.59		
	(2, 3.8, 3.2, 12, 6, 0.6, 1.8, 5, 5, 4, 348)	0.458	77.15	(2, 3.8, 4.2, 12, 6, 1.4, 1.4, 3, 5, 4, 432)	0.737	77.88		
	(2, 3.8, 3.8, 12, 6, 1.0, 1.8, 5, 5, 4, 348)	0.464	77.29	(2, 3.8, 4.2, 12, 12, 0.8, 1.2, 3, 1.5, 4, 432)	0.829	78.08		
	(2, 3.6, 3.6, 6, 12, 1.8, 2.0, 5, 2, 4, 348)	0.509	77.91	(3, 3.2, 3.6, 3.2, 6, 12, 6, 1.4, 1.8, 0.8, 3, 5, 5, 4, 480)	0.925	78.22		
Top accuracy	(2, 3.8, 3.6, 12, 12, 1.4, 2.0, 5, 2, 4, 348) ¹	0.505	77.71	(2, 3.8, 3.2, 6, 12, 0.8, 1.2, 3, 1.5, 4, 432) ¹	0.826	78.01		
	(2, 3.6, 3.6, 6, 12, 1.8, 2.0, 5, 2, 4, 348) ²	0.509	77.91	(2, 3.8, 4.2, 12, 12, 0.6, 0.8, 3, 1.5, 4, 432)	0.829	78.08		
	(2, 3.6, 3.6, 6, 12, 0.6, 2.0, 5, 2, 4, 348)	0.510	77.91	(2, 4.2, 4.2, 12, 12, 0.8, 1.2, 3, 1.5, 4, 480) ²	0.889	78.05		
	(2, 3.4, 3.8, 6, 6, 1.0, 1.8, 5, 2, 4, 360)	0.535	77.89	(3, 3.2, 3.6, 3.2, 6, 12, 6, 1.4, 1.8, 0.8, 3, 5, 5, 4, 480) ³	0.925	78.22		
	(2, 3.6, 3.6, 6, 6, 0.6, 2.0, 5, 2, 4, 360)	0.536	77.90	(3, 3.2, 3.6, 3.0, 6, 12, 12, 1.4, 2.0, 2.0, 3, 5, 3, 4, 480)	0.934	78.17		
Spikformer 4-384	(4, 4, 4, 4, 4, 12, 12, 12, 12, 1.0, 1.0, 1.0, 1.0, 2, 2, 2, 2, 4, 384)	0.95	77.86	(4, 4, 4, 4, 4, 12, 12, 12, 12, 1.0, 1.0, 1.0, 1.0, 2, 2, 2, 2, 4, 384)	0.95	77.86		

4.2 Effectiveness of ESNN

We train Auto-Spikformer within the SNN search space (\mathcal{S}_S), where only the SNN parameter sets are modified while maintaining the original Spikformer structure depicted in Table 1 (b). We select 300 candidates through the proposed ESNN and the \mathcal{F}_{AEB} . We then plot energy and accuracy for each candidate and draw a Pareto frontier. Notably, by solely modifying the SNN inner parameter sets, a superior trade-off between energy consumption and accuracy can be achieved.

There is a moderate Kendall’s tau rank correlation of 0.4 between the accuracy and the energy consumption. Some candidates exhibit lower energy consumption but higher accuracy, indicating that they are more optimal than others. The energy consumption within \mathcal{S}_S is mainly determined by the firing rate, as the architecture is fixed. We select the candidates located on the Pareto frontier, as well as a subset of candidates with the top 20% accuracy, and present them in Table 2.

We observe that our fitness function and search algorithm favor a time-step of 4, which is the maximum value in \mathcal{S}_S . Furthermore, we aim to understand why different levels of energy consumption can result in similar accuracy. We notice that the network weights of these candidates are identical. Among them, the minimum energy consumption recorded is 0.79, while the maximum energy consumption is 0.99, resulting in a 25% difference. Remarkably, despite this significant divergence in energy consumption, the corresponding accuracies achieved are nearly equivalent.

As shown in Table 2, for a similar threshold value, the firing rate decreases as the decay parameter increases. The evolutionary search tends to adjust the tau parameter rather than the threshold to control the firing rate. The decay parameter in SNN has a profound effect on the firing rate by facilitating a

Table 4: Performance comparison of Auto-Spikformer with existing methods on CIFAR10/100. Auto-Spikformer architectures $\mathcal{S}_{T_s 1,2}$ and $\mathcal{S}_{T_l 1,2,3}$ are selected from the candidate architectures listed in Table 3. Auto-Spikformer is the first transformer model designed through automated methods, demonstrating enhanced performance in both tasks. The symbol "*" denotes results obtained from self-implemented experiments by [13].

Methods	Architecture	Param (M) / Energy (μJ)	Time Step	CIFAR10 Acc	CIFAR100 Acc	Model Type	Design Type
Hybrid training[50]	VGG-11	9.27	125	92.22	67.87	CNN	Manual
Diet-SNN[48]	ResNet-20	0.27	10/5	92.54	64.07	CNN	Manual
STBP[63]	CIFARNet	17.54	12	89.83	-	CNN	Manual
STBP NeuNorm[64]	CIFARNet	17.54	12	90.53	-	CNN	Manual
TSSL-BP[73]	CIFARNet	17.54	5	91.41	-	CNN	Manual
STBP-tdBN[75]	ResNet-19	12.63	4	92.92	70.86	CNN	Manual
TET[13]	ResNet-19	12.63	4	94.44	74.47	CNN	Manual
AutoSNN[41]	AutoSNN (C=128)	21	8	93.15	69.16	CNN	Auto
SNASNet[30]	SNASNet-Bw	-	8	94.12	73.04	CNN	Auto
SpikeDHS ^D [5]	SpikeDHS-CLA (n3s1)	14	6	95.36	76.25	CNN	Auto
ANN	ResNet-19*	12.63	1	94.97	75.35	CNN	Manual
	Transformer-4-384	9.32 / 3.97	1	96.73	81.02	Transformer	Manual
Spikformer	Spikformer-4-256	4.15 / 0.553	4	93.94	75.96	Transformer	Manual
	Spikformer-2-384	5.76 / 0.582	4	94.80	76.95	Transformer	Manual
	Spikformer-4-384	9.32 / 0.952	4	95.19	77.86	Transformer	Manual
Auto-Spikformer	Auto-Spikformer $\mathcal{S}_{T_s 1}$	4.69 / 0.505	4	95.29	77.71	Transformer	Auto
	Auto-Spikformer $\mathcal{S}_{T_s 2}$	4.64 / 0.509	4	95.23	77.91	Transformer	Auto
	Auto-Spikformer $\mathcal{S}_{T_l 1}$	7.09 / 0.826	4	96.19	78.01	Transformer	Auto
	Auto-Spikformer $\mathcal{S}_{T_l 2}$	9.20 / 0.889	4	96.38	77.05	Transformer	Auto
	Auto-Spikformer $\mathcal{S}_{T_l 3}$	8.46 / 0.925	4	96.39	78.22	Transformer	Auto

memory effect for the previous membrane potential. Additionally, the decay and threshold parameters also affect the distribution of feature maps across the layers. Thus, by adjusting the tau and threshold values of each neuron, we can alter the firing rate and accuracy substantially. This shows that the proposed ESNN is a promising approach. By designing an appropriate search space and selecting a suitable fitness function, we are able to effectively decrease the overall firing rate while preserving the network’s performance.

4.3 Effectiveness of \mathcal{F}_{AEB}

To demonstrate the superiority of the \mathcal{F}_{AEB} , we conduct extensive experiments and illustrate the trade-off between energy and accuracy. We apply evolutionary search with the \mathcal{F}_{AEB} as the fitness function to generate 1000 samples in both \mathcal{S}_{T_s} and \mathcal{S}_{T_l} . Then we select the top 100 candidates based on their scores. For comparison, we also randomly sample 100 candidates from the search space. Additionally, we also include the Spikformer architecture in the energy-accuracy plot.

As shown in Figure 3, the Pareto front of the \mathcal{F}_{AEB} dominates the random sample approach. The Kendall’s tau rank correlation coefficients of evolutionary search and random sample are 0.63 and 0.08 in \mathcal{S}_{T_s} and 0.60 and 0.24 in \mathcal{S}_{T_l} , respectively. The candidates on the Pareto front are listed in Table 3 (a) and the remaining ones are provided in the supplementary materials. We observe that there are numerous candidates that achieve a favorable balance between accuracy and energy consumption. In \mathcal{S}_{T_s} , some candidates on the frontier even surpass the original 4-384 Spikformer architecture in accuracy with only 2 blocks and 348 channels, which means half of the energy consumption. \mathcal{S}_{T_l} is used to further explore higher accuracy architecture as shown in Table 3 (b). The highest accuracy is 78.22 with a lower energy consumption of 0.925 μJ . Furthermore, several candidates exhibited 10% to 25% less energy while achieving higher accuracy compared to the 4-384 Spikformer architecture.

4.4 Result on CIFAR

We select the Auto-Spikformer architecture searched in \mathcal{S}_{T_s} and \mathcal{S}_{T_l} in Section 4.3 and compare with original Spikformer and other methods. The performances are reported in Table 4. Auto-Spikformer is the first transformer model designed through automated methods. Auto-Spikformer $\mathcal{S}_{T_s 2}$ and $\mathcal{S}_{T_l 1, 2, 3}$ outperform the state-of-the-art method including CNN or Transformer models that are

manually or automatically designed in both accuracy and energy consumption. Compare to the original Spikformer, the Auto-Spikformer obtains a significant improvement of accuracy with even less energy consumption. The ANN-Transformer model is only 0.34% and 2.8 % than ST_l 1, 2, 3, respectively, which demonstrates that the Auto-Spikformer method is comparable to the ANN version.

5 Conclusion

In this work, we are the first to propose a one-shot architecture search method for spiking-based vision transformers, called Auto-Spikformer. Auto-Spikformer optimizes both energy consumption and accuracy by incorporating key parameters of SNN and transformer into the search space. We propose two novel methods: Evolutionary SNN neurons (ESNN), which optimizes the SNN parameters, and Accuracy and Energy Balanced Fitness Function \mathcal{F}_{AEB} , which balances the energy consumption and accuracy objectives. Extensive experiments show that the proposed algorithm can improve the performance of Spikformer and discover many promising architectures. As a future work, we plan to conduct experiments on larger benchmark datasets or neuromorphic datasets.

References

- [1] Tong Bu, Wei Fang, Jianhao Ding, PengLin Dai, Zhaofei Yu, and Tiejun Huang. Optimal ann-snn conversion for high-accuracy and ultra-low-latency spiking neural networks. In *International Conference on Learning Representations*, 2021.
- [2] Yongqiang Cao, Yang Chen, and Deepak Khosla. Spiking deep convolutional neural networks for energy-efficient object recognition. *International Journal of Computer Vision*, 113(1):54–66, 2015.
- [3] Nicolas Carion, Francisco Massa, Gabriel Synnaeve, Nicolas Usunier, Alexander Kirillov, and Sergey Zagoruyko. End-to-end object detection with transformers. In *Proceedings of the European Conference on Computer Vision (ECCV)*, pages 213–229. Springer, 2020.
- [4] Charlotte Caucheteux and Jean-Rémi King. Brains and algorithms partially converge in natural language processing. *Communications biology*, 5(1):1–10, 2022.
- [5] Kaiwei Che, Luziwei Leng, Kaixuan Zhang, Jianguo Zhang, Qinghu Meng, Jie Cheng, Qinghai Guo, and Jianxing Liao. Differentiable hierarchical and surrogate gradient search for spiking neural networks. *Advances in Neural Information Processing Systems*, 35:24975–24990, 2022.
- [6] Boyu Chen, Peixia Li, Chuming Li, Baopu Li, Lei Bai, Chen Lin, Ming Sun, Junjie Yan, and Wanli Ouyang. Glit: Neural architecture search for global and local image transformer. In *Proceedings of the IEEE/CVF International Conference on Computer Vision*, pages 12–21, 2021.
- [7] Minghao Chen, Houwen Peng, Jianlong Fu, and Haibin Ling. Autoformer: Searching transformers for visual recognition. In *Proceedings of the IEEE/CVF international conference on computer vision*, pages 12270–12280, 2021.
- [8] Xin Chen, Lingxi Xie, Jun Wu, and Qi Tian. Progressive differentiable architecture search: Bridging the depth gap between search and evaluation. In *Proceedings of the IEEE/CVF International Conference on Computer Vision*, pages 1294–1303, 2019.
- [9] Yukang Chen, Tong Yang, Xiangyu Zhang, Gaofeng Meng, Xinyu Xiao, and Jian Sun. Detnas: Backbone search for object detection. *Advances in Neural Information Processing Systems*, 32, 2019.
- [10] Xuelian Cheng, Yiran Zhong, Mehrtash Harandi, Yuchao Dai, Xiaojun Chang, Hongdong Li, Tom Drummond, and Zongyuan Ge. Hierarchical neural architecture search for deep stereo matching. *Advances in Neural Information Processing Systems*, 33:22158–22169, 2020.
- [11] Krzysztof Choromanski, Valerii Likhoshesterov, David Dohan, Xingyou Song, Andreea Gane, Tamas Sarlos, Peter Hawkins, Jared Davis, Afroz Mohiuddin, Lukasz Kaiser, et al. Rethinking attention with performers. *arXiv preprint arXiv:2009.14794*, 2020.

- [12] Xiangxiang Chu, Xiaoxing Wang, Bo Zhang, Shun Lu, Xiaolin Wei, and Junchi Yan. Darts-: robustly stepping out of performance collapse without indicators. *arXiv preprint arXiv:2009.01027*, 2020.
- [13] Shikuang Deng, Yuhang Li, Shanghang Zhang, and Shi Gu. Temporal efficient training of spiking neural network via gradient re-weighting. *arXiv preprint arXiv:2202.11946*, 2022.
- [14] Xuanyi Dong and Yi Yang. One-shot neural architecture search via self-evaluated template network. In *Proceedings of the IEEE/CVF International Conference on Computer Vision*, pages 3681–3690, 2019.
- [15] Alexey Dosovitskiy, Lucas Beyer, Alexander Kolesnikov, Dirk Weissenborn, Xiaohua Zhai, Thomas Unterthiner, Mostafa Dehghani, Matthias Minderer, Georg Heigold, Sylvain Gelly, et al. An image is worth 16x16 words: Transformers for image recognition at scale. *arXiv preprint arXiv:2010.11929*, 2020.
- [16] Thomas Elsken, Jan Hendrik Metzen, and Frank Hutter. Neural architecture search: A survey. *The Journal of Machine Learning Research*, 20(1):1997–2017, 2019.
- [17] Wei Fang, Zhaofei Yu, Yanqi Chen, Tiejun Huang, Timothée Masquelier, and Yonghong Tian. Deep residual learning in spiking neural networks. *Advances in Neural Information Processing Systems*, 34, 2021.
- [18] Wei Fang, Zhaofei Yu, Yanqi Chen, Timothée Masquelier, Tiejun Huang, and Yonghong Tian. Incorporating learnable membrane time constant to enhance learning of spiking neural networks. In *Proceedings of the IEEE/CVF International Conference on Computer Vision*, pages 2661–2671, 2021.
- [19] Bertrand Fontaine, José Luis Peña, and Romain Brette. Spike-threshold adaptation predicted by membrane potential dynamics in vivo. *PLoS computational biology*, 10(4):e1003560, 2014.
- [20] Jianyuan Guo, Kai Han, Yunhe Wang, Chao Zhang, Zhaohui Yang, Han Wu, Xinghao Chen, and Chang Xu. Hit-detector: Hierarchical trinity architecture search for object detection. In *Proceedings of the IEEE/CVF Conference on Computer Vision and Pattern Recognition*, pages 11405–11414, 2020.
- [21] Bing Han, Gopalakrishnan Srinivasan, and Kaushik Roy. Rmp-snn: Residual membrane potential neuron for enabling deeper high-accuracy and low-latency spiking neural network. In *Proceedings of the IEEE/CVF Conference on Computer Vision and Pattern Recognition (CVPR)*, pages 13558–13567, 2020.
- [22] Ali Hassani, Steven Walton, Nikhil Shah, Abulikemu Abuduweili, Jiachen Li, and Humphrey Shi. Escaping the big data paradigm with compact transformers. *arXiv preprint arXiv:2104.05704*, 2021.
- [23] Kaiming He, Xinlei Chen, Saining Xie, Yanghao Li, Piotr Dollár, and Ross Girshick. Masked autoencoders are scalable vision learners. In *Proceedings of the IEEE/CVF Conference on Computer Vision and Pattern Recognition*, pages 16000–16009, 2022.
- [24] Mark Horowitz. 1.1 computing’s energy problem (and what we can do about it). In *2014 IEEE International Solid-State Circuits Conference Digest of Technical Papers (ISSCC)*, pages 10–14. IEEE, 2014.
- [25] Yangfan Hu, Huajin Tang, and Gang Pan. Spiking deep residual networks. *IEEE Transactions on Neural Networks and Learning Systems*, pages 1–6, 2021. doi: 10.1109/TNNLS.2021.3119238.
- [26] Yifan Hu, Yujie Wu, Lei Deng, and Guoqi Li. Advancing residual learning towards powerful deep spiking neural networks. *arXiv preprint arXiv:2112.08954*, 2021.
- [27] Eric Hunsberger and Chris Eliasmith. Spiking deep networks with lif neurons. *arXiv preprint arXiv:1510.08829*, 2015.
- [28] Jakob Jordan, Maximilian Schmidt, Walter Senn, and Mihai A Petrovici. Evolving interpretable plasticity for spiking networks. *Elife*, 10:e66273, 2021.

- [29] Angelos Katharopoulos, Apoorv Vyas, Nikolaos Pappas, and François Fleuret. Transformers are rnns: Fast autoregressive transformers with linear attention. In *Proceedings of the 37th International Conference on Machine Learning (ICML)*, pages 5156–5165, 2020.
- [30] Youngeun Kim, Yuhang Li, Hyoungseob Park, Yeshwanth Venkatesha, and Priyadarshini Panda. Neural architecture search for spiking neural networks. *arXiv preprint arXiv:2201.10355*, 2022.
- [31] Souvik Kundu, Gourav Datta, Massoud Pedram, and Peter A Beerel. Spike-thrift: Towards energy-efficient deep spiking neural networks by limiting spiking activity via attention-guided compression. In *Proceedings of the IEEE/CVF Winter Conference on Applications of Computer Vision (WACV)*, pages 3953–3962, 2021.
- [32] Souvik Kundu, Massoud Pedram, and Peter A Beerel. Hire-snn: Harnessing the inherent robustness of energy-efficient deep spiking neural networks by training with crafted input noise. In *Proceedings of the IEEE/CVF International Conference on Computer Vision (ICCV)*, pages 5209–5218, 2021.
- [33] Chankyu Lee, Syed Shakib Sarwar, Priyadarshini Panda, Gopalakrishnan Srinivasan, and Kaushik Roy. Enabling spike-based backpropagation for training deep neural network architectures. *Frontiers in neuroscience*, 14:119, 2020.
- [34] Peiwen Lin, Peng Sun, Guangliang Cheng, Sirui Xie, Xi Li, and Jianping Shi. Graph-guided architecture search for real-time semantic segmentation. In *Proceedings of the IEEE/CVF Conference on Computer Vision and Pattern Recognition*, pages 4203–4212, 2020.
- [35] Chenxi Liu, Barret Zoph, Maxim Neumann, Jonathon Shlens, Wei Hua, Li-Jia Li, Li Fei-Fei, Alan Yuille, Jonathan Huang, and Kevin Murphy. Progressive neural architecture search. In *Proceedings of the European conference on computer vision (ECCV)*, pages 19–34, 2018.
- [36] Chenxi Liu, Liang-Chieh Chen, Florian Schroff, Hartwig Adam, Wei Hua, Alan L Yuille, and Li Fei-Fei. Auto-deeplab: Hierarchical neural architecture search for semantic image segmentation. In *Proceedings of the IEEE/CVF conference on computer vision and pattern recognition*, pages 82–92, 2019.
- [37] Hanxiao Liu, Karen Simonyan, and Yiming Yang. Darts: Differentiable architecture search. *arXiv preprint arXiv:1806.09055*, 2018.
- [38] Ze Liu, Yutong Lin, Yue Cao, Han Hu, Yixuan Wei, Zheng Zhang, Stephen Lin, and Baining Guo. Swin transformer: Hierarchical vision transformer using shifted windows. In *Proceedings of the IEEE/CVF International Conference on Computer Vision (ICCV)*, pages 10012–10022, 2021.
- [39] Ali Lotfi Rezaabad and Sriram Vishwanath. Long short-term memory spiking networks and their applications. In *Proceedings of the International Conference on Neuromorphic Systems 2020 (ICONS)*, pages 1–9, 2020.
- [40] Qingyan Meng, Mingqing Xiao, Shen Yan, Yisen Wang, Zhouchen Lin, and Zhi-Quan Luo. Training High-Performance Low-Latency Spiking Neural Networks by Differentiation on Spike Representation. *ArXiv preprint arXiv:2205.00459*, 2022.
- [41] Byunggook Na, Jisoo Mok, Seongsik Park, Dongjin Lee, Hyeokjun Choe, and Sungroh Yoon. Autosnn: Towards energy-efficient spiking neural networks. *arXiv preprint arXiv:2201.12738*, 2022.
- [42] Emre O Neftci, Hesham Mostafa, and Friedemann Zenke. Surrogate gradient learning in spiking neural networks: Bringing the power of gradient-based optimization to spiking neural networks. *IEEE Signal Processing Magazine*, 36(6):51–63, 2019.
- [43] Vladimir Nekrasov, Hao Chen, Chunhua Shen, and Ian Reid. Fast neural architecture search of compact semantic segmentation models via auxiliary cells. In *Proceedings of the IEEE/CVF conference on computer vision and pattern recognition*, pages 9126–9135, 2019.

- [44] Priyadarshini Panda, Sai Aparna Aketi, and Kaushik Roy. Toward scalable, efficient, and accurate deep spiking neural networks with backward residual connections, stochastic softmax, and hybridization. *Frontiers in Neuroscience*, 14:653, 2020.
- [45] Hieu Pham, Melody Guan, Barret Zoph, Quoc Le, and Jeff Dean. Efficient neural architecture search via parameters sharing. In *International conference on machine learning*, pages 4095–4104. PMLR, 2018.
- [46] Zhen Qin, Weixuan Sun, Hui Deng, Dongxu Li, Yunshen Wei, Baohong Lv, Junjie Yan, Lingpeng Kong, and Yiran Zhong. cosformer: Rethinking softmax in attention. *arXiv preprint arXiv:2202.08791*, 2022.
- [47] Yongming Rao, Wenliang Zhao, Benlin Liu, Jiwen Lu, Jie Zhou, and Cho-Jui Hsieh. Dynamicvit: Efficient vision transformers with dynamic token sparsification. In *Proceedings of the International Conference on Neural Information Processing Systems (NeurIPS)*, volume 34, pages 13937–13949, 2021.
- [48] Nitin Rathi and Kaushik Roy. Diet-snn: Direct input encoding with leakage and threshold optimization in deep spiking neural networks. *arXiv preprint arXiv:2008.03658*, 2020.
- [49] Nitin Rathi and Kaushik Roy. Diet-snn: A low-latency spiking neural network with direct input encoding and leakage and threshold optimization. *IEEE Transactions on Neural Networks and Learning Systems*, 2021.
- [50] Nitin Rathi, Gopalakrishnan Srinivasan, Priyadarshini Panda, and Kaushik Roy. Enabling deep spiking neural networks with hybrid conversion and spike timing dependent backpropagation. *arXiv preprint arXiv:2005.01807*, 2020.
- [51] Esteban Real, Alok Aggarwal, Yanping Huang, and Quoc V Le. Regularized evolution for image classifier architecture search. In *Proceedings of the aaai conference on artificial intelligence*, volume 33, pages 4780–4789, 2019.
- [52] Bodo Rueckauer, Iulia-Alexandra Lungu, Yuhuang Hu, Michael Pfeiffer, and Shih-Chii Liu. Conversion of continuous-valued deep networks to efficient event-driven networks for image classification. *Frontiers in neuroscience*, 11:682, 2017.
- [53] Adam Slowik and Halina Kwasnicka. Evolutionary algorithms and their applications to engineering problems. *Neural Computing and Applications*, 32:12363–12379, 2020.
- [54] Jeong-geun Song. Ufo-vit: High performance linear vision transformer without softmax. *arXiv preprint arXiv:2109.14382*, 2021.
- [55] Xiu Su, Shan You, Jiyang Xie, Mingkai Zheng, Fei Wang, Chen Qian, Changshui Zhang, Xiaogang Wang, and Chang Xu. Vitas: Vision transformer architecture search. In *Computer Vision—ECCV 2022: 17th European Conference, Tel Aviv, Israel, October 23–27, 2022, Proceedings, Part XXI*, pages 139–157. Springer, 2022.
- [56] Hugo Touvron, Matthieu Cord, Matthijs Douze, Francisco Massa, Alexandre Sablayrolles, and Hervé Jégou. Training data-efficient image transformers & distillation through attention. In *International conference on machine learning*, pages 10347–10357. PMLR, 2021.
- [57] Ashish Vaswani, Noam Shazeer, Niki Parmar, Jakob Uszkoreit, Llion Jones, Aidan N Gomez, Łukasz Kaiser, and Illia Polosukhin. Attention is all you need. In *Proceedings of the International Conference on Neural Information Processing Systems (NeurIPS)*, volume 30, 2017.
- [58] Ning Wang, Yang Gao, Hao Chen, Peng Wang, Zhi Tian, Chunhua Shen, and Yanning Zhang. Nas-fcos: Fast neural architecture search for object detection. In *Proceedings of the IEEE/CVF Conference on Computer Vision and Pattern Recognition*, pages 11943–11951, 2020.
- [59] Wenhai Wang, Enze Xie, Xiang Li, Deng-Ping Fan, Kaitao Song, Ding Liang, Tong Lu, Ping Luo, and Ling Shao. Pyramid vision transformer: A versatile backbone for dense prediction without convolutions. In *Proceedings of the IEEE/CVF International Conference on Computer Vision (ICCV)*, pages 568–578, 2021.

- [60] Yuchen Wang, Malu Zhang, Yi Chen, and Hong Qu. Signed neuron with memory: Towards simple, accurate and high-efficient ann-snn conversion. In *International Joint Conference on Artificial Intelligence*, 2022.
- [61] Paul J Werbos. Backpropagation through time: what it does and how to do it. *Proceedings of the IEEE*, 78(10):1550–1560, 1990.
- [62] James C. R. Whittington, Joseph Warren, and Tim E.J. Behrens. Relating transformers to models and neural representations of the hippocampal formation. In *International Conference on Learning Representations (ICLR)*, 2022. URL <https://openreview.net/forum?id=B8DVo9B1YE0>.
- [63] Yujie Wu, Lei Deng, Guoqi Li, Jun Zhu, and Luping Shi. Spatio-temporal backpropagation for training high-performance spiking neural networks. *Frontiers in neuroscience*, 12:331, 2018.
- [64] Yujie Wu, Lei Deng, Guoqi Li, Jun Zhu, Yuan Xie, and Luping Shi. Direct training for spiking neural networks: Faster, larger, better. In *Proceedings of the AAAI Conference on Artificial Intelligence*, volume 33, pages 1311–1318, 2019.
- [65] Mingqing Xiao, Qingyan Meng, Zongpeng Zhang, Yisen Wang, and Zhouchen Lin. Training feedback spiking neural networks by implicit differentiation on the equilibrium state. volume 34, pages 14516–14528, 2021.
- [66] Tete Xiao, Mannat Singh, Eric Mintun, Trevor Darrell, Piotr Dollár, and Ross Girshick. Early convolutions help transformers see better. In *Proceedings of the International Conference on Neural Information Processing Systems (NeurIPS)*, volume 34, pages 30392–30400, 2021.
- [67] Yuhui Xu, Lingxi Xie, Xiaopeng Zhang, Xin Chen, Guo-Jun Qi, Qi Tian, and Hongkai Xiong. Pc-darts: Partial channel connections for memory-efficient architecture search. *arXiv preprint arXiv:1907.05737*, 2019.
- [68] Jianwei Yang, Chunyuan Li, Pengchuan Zhang, Xiyang Dai, Bin Xiao, Lu Yuan, and Jianfeng Gao. Focal attention for long-range interactions in vision transformers. In *Proceedings of the International Conference on Neural Information Processing Systems (NeurIPS)*, volume 34, pages 30008–30022, 2021.
- [69] Man Yao, Guangshe Zhao, Hengyu Zhang, Yifan Hu, Lei Deng, Yonghong Tian, Bo Xu, and Guoqi Li. Attention spiking neural networks. *arXiv preprint arXiv:2209.13929*, 2022.
- [70] Bojian Yin, Federico Corradi, and Sander M Bohté. Accurate and efficient time-domain classification with adaptive spiking recurrent neural networks. *Nature Machine Intelligence*, 3(10):905–913, 2021.
- [71] Li Yuan, Yunpeng Chen, Tao Wang, Weihao Yu, Yujun Shi, Zi-Hang Jiang, Francis EH Tay, Jiashi Feng, and Shuicheng Yan. Tokens-to-token vit: Training vision transformers from scratch on imagenet. In *Proceedings of the IEEE/CVF International Conference on Computer Vision (ICCV)*, pages 558–567, 2021.
- [72] Li Yuan, Qibin Hou, Zihang Jiang, Jiashi Feng, and Shuicheng Yan. Volo: Vision outlooker for visual recognition. *arXiv preprint arXiv:2106.13112*, 2021.
- [73] Wenrui Zhang and Peng Li. Temporal spike sequence learning via backpropagation for deep spiking neural networks. *Advances in Neural Information Processing Systems*, 33:12022–12033, 2020.
- [74] Yiheng Zhang, Zhaofan Qiu, Jingen Liu, Ting Yao, Dong Liu, and Tao Mei. Customizable architecture search for semantic segmentation. In *Proceedings of the IEEE/CVF Conference on Computer Vision and Pattern Recognition*, pages 11641–11650, 2019.
- [75] Hanle Zheng, Yujie Wu, Lei Deng, Yifan Hu, and Guoqi Li. Going deeper with directly-trained larger spiking neural networks. In *Proceedings of the AAAI Conference on Artificial Intelligence*, volume 35, pages 11062–11070, 2021.

- [76] Zhaokun Zhou, Yuesheng Zhu, Chao He, Yaowei Wang, Shuicheng Yan, Yonghong Tian, and Li Yuan. Spikformer: When spiking neural network meets transformer, 2022.
- [77] Xizhou Zhu, Weijie Su, Lewei Lu, Bin Li, Xiaogang Wang, and Jifeng Dai. Deformable detr: Deformable transformers for end-to-end object detection. *arXiv preprint arXiv:2010.04159*, 2020.
- [78] Barret Zoph and Quoc V Le. Neural architecture search with reinforcement learning. *arXiv preprint arXiv:1611.01578*, 2016.
- [79] Barret Zoph, Vijay Vasudevan, Jonathon Shlens, and Quoc V Le. Learning transferable architectures for scalable image recognition. In *Proceedings of the IEEE conference on computer vision and pattern recognition*, pages 8697–8710, 2018.